NFMCC Technical Note – 549
Revised 3 June 2010

Low-beta bucked coil cooling channels

R.C. Fernow
Brookhaven National Laboratory

8 April 2010

We examine the use of low-beta bucked coil lattices for 6D and final cooling for the muon collider. A straight tapered channel cools the transverse normalized emittance from 1.01 to 0.12 mm with 34% transmission. Possible causes for the large transmission losses are examined. Using a matrix transformation corresponding to ideal emittance exchange only increased the transmission to 37%. Ring configurations examined so far have worse performance.

1. Introduction

An examination of the properties of solenoidal cooling lattices [1,2] revealed the existence of a class of lattices that could produce very small beta functions for a given magnetic field strength on-axis. This is expressed quantitatively by comparing the beta function in the lattice to that produced by a continuous solenoid

$$F_1 = \frac{\beta}{\beta_o} = \frac{eB_o\beta}{2p}$$

where B_o is the peak on-axis solenoid field. Solutions were found with F_1~0.2 with the minimum of the beta function at the midplane of the solenoid magnet. Palmer subsequently suggested designs [3] that surrounded the focusing solenoid with *bucking coils* in order to greatly reduce the magnetic field present on the RF cavities. Low-beta lattices of this type were also investigated by Alexahin [4] and by Fernow. We will discuss some properties of these designs in section 7.

We will refer to lattices of this type as low-beta bucked coil (**LBBC**) lattices. For the purpose of this report low beta means ≤ 5 cm. A generic cell of the simplest type of this lattice is shown in Fig. 1.

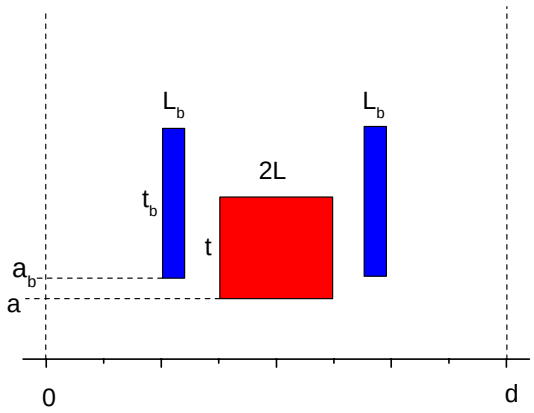

Figure 1. One cell of an LBBC lattice.

In this report we will examine the possibility of replacing part of the 6D or final cooling in the HEMC cooling scenario [5] with an LBBC lattice.

Related studies have also examined using larger beta (75-150 cm) bucked solutions for the neutrino factory [6]. Recently Rogers [7] has studied the properties of iron shielded lattices for use in a neutrino factory.

2. Basic properties of LBBC lattices

LBBC lattices operate in the second momentum passband. The central momentum p_2 of this passband is proportional to the product of the peak field on-axis B_o and the cell length d

$$p_2 \propto B_o d$$

The width of the passband is proportional to the momentum

$$\Delta p_2 \propto p_2$$

The minimum value of the beta function is proportional to the momentum and inversely proportional to the peak on-axis field

$$\beta_{\min} \propto \frac{p_2}{B_o}$$

The beta function for these lattices grows rapidly from the minimum at the center of the focusing solenoid.

For optimum cooling the absorber length L_{abs} should satisfy

$$L_{abs} < 2\,\beta_{\min}$$

The average beta function over the absorber is given by

$$\beta_{abs} = \frac{1}{L}\int_0^L \left[\beta^* + \frac{z^2}{\beta^*}\right] dz = \beta^* + \frac{L^2}{3\beta^*}$$

where L is the half-length of the absorber and $\beta^* = \beta_{\min}$.

We assumed the maximum RF gradient available was given by

$$G[MV/m] = 1.4\sqrt{f\,[MHz]}$$

The maximum initial cooling rate (%/m) in the channel is defined by

$$icr = \frac{\frac{dE}{dz} L_{abs}}{d\ E_{ref}}$$

The on-axis magnetic field is shown for a typical LBBC lattice in Fig. 2.

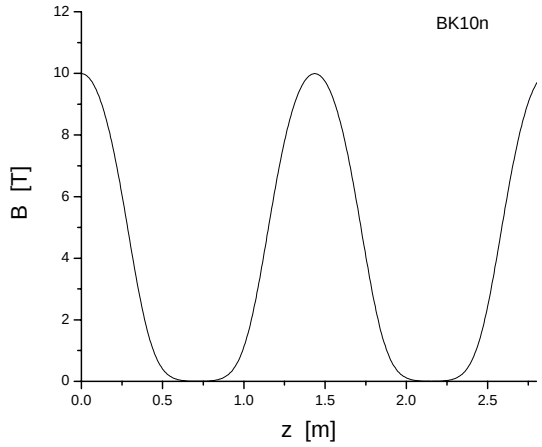

Figure 2. On-axis magnetic field for two cells of the BK10n lattice.

3. The LBBC cooling scenario

The parts of the HEMC scenario where it would be interesting to consider using LBBC lattices range from the beginning of the 805 MHz Guggenheim channel to roughly the middle of the 50 T final cooling channel. The transverse normalized emittances that are used here range from ~1.1 to 0.1 mm and the corresponding longitudinal normalized emittances have values ~ 2 to 5 mm.

Table 1 shows the solenoid properties for six LBBC lattices (models BK) whose peak field on-axis increases in roughly 5 T intervals. The column labels are defined in Fig. 1.

Table 1 Solenoid properties

model	d	2L	a	t	J	z_b	L_b	a_b	t_b	J_b
	[cm]	[cm]	[cm]	[cm]	[A/mm^2]	[cm]	[cm]	[cm]	[cm]	[A/mm^2]
BK5k	284	116	36.7	27	21.3	73	18	39.8	35	-17.4
BK10n	143.6	58.1	18.3	35.1	41.94	36.7	9.2	20.2	40.9	-53.2
BK15f	94	38	12	23	97.9	24	6	13.2	26.8	-125
BK20f	71.9	29.1	9.2	17.6	167.3	18.4	4.6	10.1	20.5	-213.6
BK25e	56	22.4	6.7	13.8	268.7	14.2	3.6	8	16.2	-321.3
BK30a	48.5	19.4	6.2	11.9	370.3	12.4	3.1	6.8	13.8	-468.2
OC7a	143.6	58.1	18.3	35.1	24.8					
OC8c	143.6	58.1	18.3	35.1	±30.3					

The lattices for 10-30 T roughly scale geometrically. However, following this scaling down to 5 T requires an ugly coil with a very large radial thickness and a very small current density. For that reason this coil was reoptimized. Models OC7a and OC8c are non-bucked one-coil-per cell lattices that will be discussed later in connection with losses.

We assume an operating momentum of 200 MeV/c for all of these lattices. The beta function for the 10 T lattice is shown in Fig. 3.

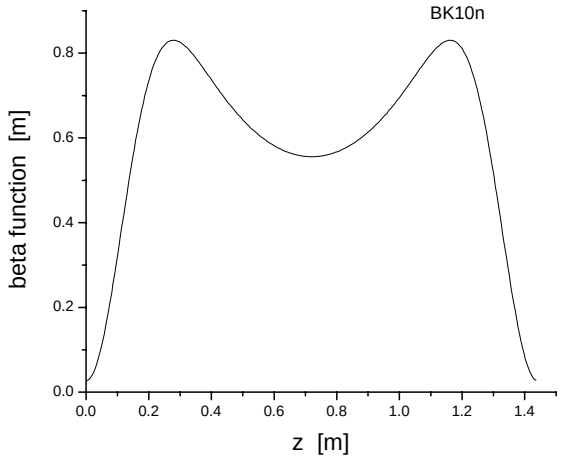

Figure 3. Beta function versus distance in the BK10n lattice.

The maximum value of the beta function occurs near the end of the focusing solenoid. The shape of the beta function is similar for the other lattices in Table 1.

Some general properties for these lattices are given in Table 2.

Table 2 Lattice properties

model	B_o	Δp_2	β_{min}	β_{max}	β_{RF}	F_1
	[T]	[MeV/c]	[cm]	[cm]	[cm]	
BK5k	5.0	40	5.16	168	113	0.194
BK10n	10.0	41	2.72	83	56	0.204
BK15f	15.3	42	1.80	54	37	0.207
BK20f	19.9	42	1.36	42	28	0.203
BK25e	25.4	42	1.07	32	22	0.204
BK30a	29.7	42	0.91	28.2	19.0	0.203
OC7a	7.4	75	7.70	59	58	0.427
OB8c	8.3	57	4.83	69	54	0.301

For the BK set of lattices the central momentum of the passband is given by

$$p_2\ [MeV/c] \approx 14.1\ B_o[T]\ d\ [m]$$

The width of the passband is given by

$$\frac{\Delta p_2}{p_2} \approx \pm 0.10$$

Note that the momentum acceptance Δp_2 stays constant as the beta function is reduced.

The minimum value of the beta function is given by

$$\beta_{\min}\ [cm] \approx 0.135\ \frac{p_2\,[MeV/c]}{B_o\ [T]}$$

4. Straight channels

We prepared cooling channels based on each of the six BK reference lattices discussed above. Scans of RF frequency were done to maximize the transmission to obtain a specified transverse emittance. The scan for the 10 T lattice is shown in Fig. 4.

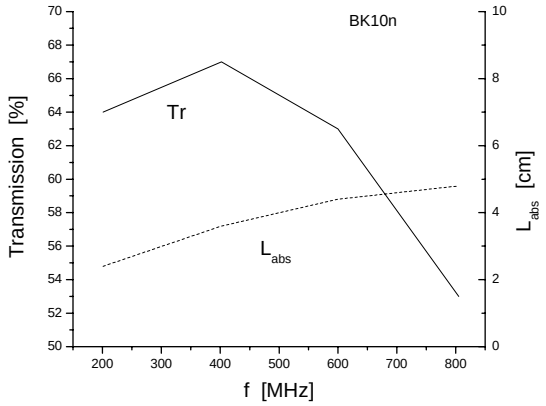

Figure 4. Transmission and absorber length versus frequency.

The transmission was determined to the point where the transverse emittance was reduced to 0.38 mm. The RF gradient was scaled with frequency and the absorber length was adjusted to keep the momentum at the end of the cell constant.

Some parameters for the cooling channels are given in Table 3.

Table 3 Cooling channel parameters

model	f_{RF}	G_{RF}	Φ_s	L_{RF}	L_{abs}	β_{abs}	icr	ε_{eq}	ε_i	ε_f
	[MHz]	[MV/m]	[°]	[cm]	[cm]	[cm]	[%/m]	[μm]	[μm]	[μm]
BK5k	402	26	30	90	10.2	6.84	2.5	417	1250	835
BK10n	402	26	30	41.8	3.6	3.12	1.8	190	570	380
BK15f	402	26	30	26	2.2	2.02	1.7	123	370	250
BK20f	300	22	30	19.9	1.4	1.48	1.4	90	270	180
BK25e	300	22	30	14.4	1.0	1.15	1.3	70	210	140
BK30a	300	22	30	11.5	0.74	0.96	1.1	59	180	120

Because of the small beta functions we will use LiH as the absorber in the cooling lattices. ε_{eq} is the equilibrium transverse normalized emittance that can be achieved in each lattice. ε_i is the initial emittance for the channel, which is taken as ~3 times the equilibrium value in order to get a good initial rate of cooling. We stop using a channel when the emittance reaches ε_f, which we take as ~2 times the equilibrium value in order to avoid the exponential approach of the emittance to the equilibrium value. Note that the initial cooling rate is rapidly decreasing as the field increases, so that 30 T is probably the practical limit for scaled values of this particular design.

Although decreasing the RF frequency helps the problem of particles falling out of the bucket, the reduced gradient requires that the absorber thickness be reduced below the amount required by the minimum of the beta function.

The maximum initial cooling rate in the 5 T and 10 T lattices are similar to those for other cooling channels like Study 2/MICE (*icr* = 1.9%/m) or Study 2a (*icr* = 1.8%/m). However, the rate falls significantly for the higher field channels.

The cooling performance for the straight lattices is given in Table 4.

Table 4 Straight lattice cooling performance

model	N_{cell}	ε_{TN}	ε_{LN}	Tr
		[mm]	[mm]	[%]
BK5k	24	1.26 → 0.57	2.4 → 5.5	55
BK10n	45	1.00 → 0.38	2.1 → 3.4	66
BK15f	47	0.50 → 0.25	3.5 → 3.8	71
BK20f	54	0.36 → 0.18	3.8 → 4.0	70
BK25e	89	0.25 → 0.13	4.1 → 4.5	70
BK30a	107	0.22 → 0.12	4.0 → 4.5	66
OC7a	45	1.00 → 0.61	2.1 → 3.9	94
OC8c	45	1.00 → 0.49	2.1 → 4.0	90

The OC lattices used the same absorbers and RF cavities as the BK10n lattice. All the channels cool transversely with a small growth of longitudinal emittance.[1] However, there are significant problems with losses in the bucked channels.

We next combine the BK lattices into a single *tapered* channel. There doesn't appear to be any reason for using the BK5k channel since the BK10n channel covers its cooling range with better transmission. Likewise the BK30a channel doesn't give any significant advantage over the BK25e channel. Therefore we put together the tapered channel given in Table 5.

Table 5 Tapered cooling channel performance

model	N_{cell}	length	ε_{TN}	ε_{LN}	Tr
		[m]	[mm]	[mm]	[%]
BK10n	45	64.62	0.38	3.4	67.3
BK15f	49	46.06	0.24	3.9	73.8
BK20f	36	25.88	0.18	4.5	87.3
BK25e	83	46.48	0.12	5.1	78.8
Total		**183.0**	**1.01 → 0.12**	**2.0 →5.1**	**34**

For this simulation the beam at the end of each section is fed directly into the beginning of the following section.

[1] This assumes proper matching has removed the initial jump in emittance seen with Gaussian simulations.

These simulations did not include any special matching sections. Figures 5 and 6 show the cooling channel performance.

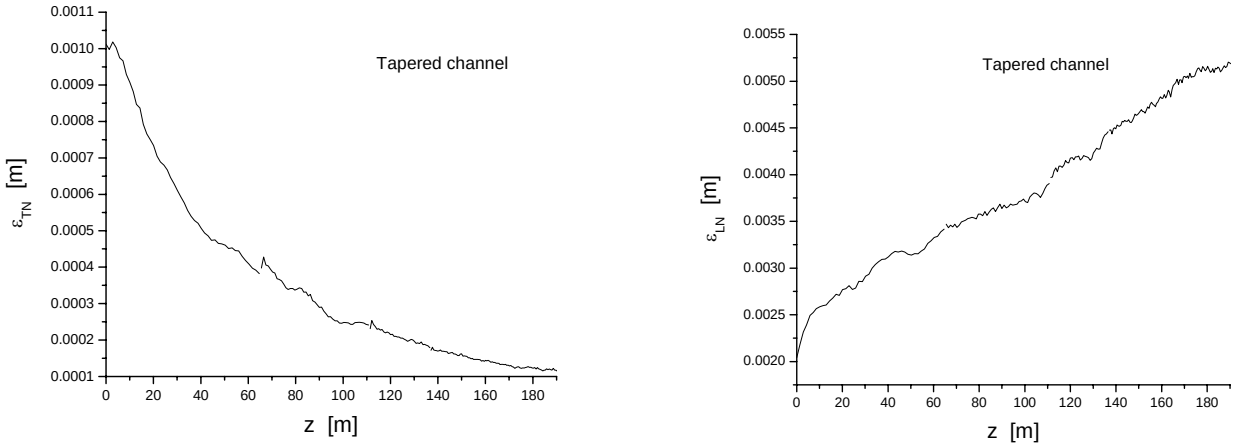

Figure 5. Normalized emittance along the tapered channel.

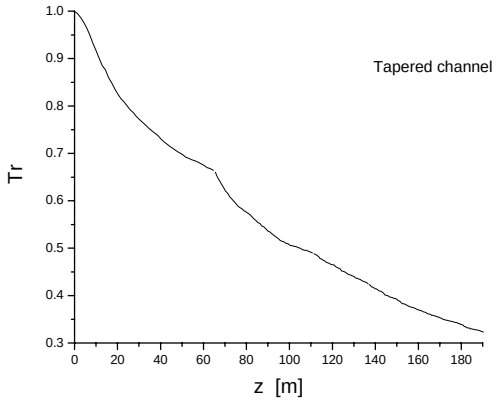

Figure 6. Transmission along the tapered channel.

We see that the channel reduces the transverse emittance from 1.00 to 0.12 mm, while the longitudinal emittance grows from 2.0 to 5.1 mm. The transmission including decays was 34%. There are small discontinuities in the emittances that could be smoothed out with special matching sections. Proper matching could probably increase the transmission to ~50%. We will discuss the losses in more detail in the following section.

5. Transmission losses

Transmission losses have been a problem in all the studies of LBBC cooling channels. For the straight channels we know that longitudinal phase space heating causes the particles to fill up the available RF bucket and eventually spill out. These particles then lose energy, become mismatched with the focusing fields, and get lost on radial apertures.

Another potential problem in these channels is the extremely rapid variation of the magnetic field caused by the bucking coils. This can lead to aberrations in the transverse focusing that can also cause losses on radial apertures. We examine the sources of particles losses in more detail in this section.

While designing these lattices we sometimes attempted to adjust the scaled design values to whole-number dimensions for convenience. The changes were compensated by adjusting the current densities, resulting in similar passband, beta function and momentum acceptance as the scaled channel. We subsequently discovered that this procedure can lead to several percent loss in transmission for simulations with the same input beam parameters.

Transverse losses

Some potential causes of losses can be avoided with proper choice of coil dimensions. Geometrical limits on the *acceptance* come from radial apertures in the focusing solenoid and in the RF cavities. The number of sigmas that can be accepted inside the focusing coil is

$$N_\sigma = a\sqrt{\frac{\beta\gamma}{\beta_{\max}\varepsilon_{TN}}}$$

The acceptance is also limited by the maximum divergence *a/L* of the beam at the center of the focusing solenoid

$$N_{\sigma'} = \frac{a}{L}\sqrt{\frac{\beta\gamma\beta_{\min}}{\varepsilon_{TN}}}$$

The acceptance inside the pillbox RF cavities is determined by the radius of the pillbox cavities

$$r_{cav} \approx 0.38\,\lambda_{RF}$$

and the *rms* beam size

$$N_{RF} = r_{cav}\sqrt{\frac{\beta\gamma}{\beta_{RF}\,\varepsilon_{TN}}}$$

These losses could be minimized by using lower frequency RF cavities. The acceptance parameters are $N_\sigma \sim 11$, $N_{\sigma'} \sim 6$, and $N_{RF} > 10$ for all of these channels, so the channel acceptance is typically limited by the divergence requirement.

The sharp fall-off of the magnetic field raises concerns about *aberrations* in the solenoidal focusing. The equation of motion in a solenoidal channel is given by

$$r'' + \kappa r = 0$$

where the focusing parameter

$$\kappa(z) = \left(\frac{e\, B_z(z)}{2\, p} \right)^2$$

varies along the channel. Variations in the solenoidal field strength or the momentum cause a change in the focusing strength

$$d\kappa = \left(\frac{e\, B_0}{2\, p_0} \right) \left[\frac{e}{p_0}\, dB - \frac{e\, B_0}{p_0^2}\, dp \right]$$

where p_0 is the reference momentum and $B_0(z)$ is the on-axis solenoidal field. The solenoid field seen by off-axis particles is

$$B_z(z, r) \approx B_0(z) - \tfrac{1}{4}\, r^2\, \frac{\partial^2\, B_0}{\partial\, z^2}$$

The focal length is related to the focusing strength by

$$\frac{1}{f} = \int \left(\kappa_0 + \delta\kappa_{sph} + \delta\kappa_{chr} \right) dz$$

where κ_0 is the focusing due to the on-axis field, $\delta\kappa_{sph}$ is the focusing error due to spherical aberrations and $\delta\kappa_{chr}$ is the focusing error due to chromatic aberrations. Thus we have the effective inverse focal length for the main focusing

$$\frac{1}{f_0} = \frac{e^2}{4\, p_0^2} \int B_0^2(z)\, dz$$

and for the spherical aberration

$$\frac{1}{f_{sph}} = \frac{e^2\, r^2}{8\, p_0} \int B_0(z)\, B''(z)\, dz$$

Note that the error is proportional to r^2 and varies across the beam distribution. The effective inverse focal length for the chromatic aberration is

$$\frac{1}{f_{chr}} = -\frac{e^2}{2\, p_0^2} \left(\frac{\delta p}{p_0} \right) \int B_0^2(z)\, dz$$

Estimates for the aberrations for these lattices are given in Table 6.

Table 6. Aberrations

model	I_1	I_2	a/2	$1/f_0$	$1/f_{sph}$	$1/f_{chr}$
	$[T^2\ m]$	$[T^2/m]$	[cm]	$[m^{-1}]$	$[m^{-1}]$	$[m^{-1}]$
BK5k	21.63	-63.0	18.3	12.2	0.1	2.4
BK10n	46.18	-485.4	9.1	25.6	0.2	5.3
BK15f	71.75	-1761	6.0	40.0	0.4	8.3
BK20f	91.95	-3861	4.6	52.6	0.5	10.3
BK25e	101.1	-6908	3.3	55.6	0.5	11.4
BK30a	135.2	-12560	3.1	76.9	0.7	15.2

I_1 is the integral of B^2 and I_2 is the integral of BB'' over one cell. We use a radius of half the inner radius of the focusing solenoid to estimate the spherical aberration. We see that the effects of spherical aberrations from beam size should be small. However, spherical aberrations due to beam divergence could be important. Using a typical momentum spread of 10% we find that chromatic aberrations are significant and smear out the focal length by ~20%.

Another way of examining the effect of the rapid field variation caused by the bucking coils is to compare with results with the bucking coils turned off. We took the BK10n lattice as an example. Removing the bucking coils leads to a one-coil-per cell lattice [2]. The OC7a single-polarity lattice in Tables 1 and 2 has the same dimensions as BK10n, but has the bucking coils removed. The current density had to be adjusted to recenter the momentum of the passband to 200 MeV/c. The resulting beta function under the coil grew with the bucking coils removed and the shape of the initial transverse phase space was corrected accordingly. The results of sending the same emittance beam through the same number of cells given in Table 4 shows that the transmission rose from 66 to 94%. One effect of changing the field profile was to increase the width of the momentum passband from 41 to 75 MeV/c. The OC8c lattice is similar, except that the polarity of the coils alternate. The transmission for OC8c was 90%. These results show that the rapid field variation is directly related to the loss in transmission.

Longitudinal losses

We found that the straight channels had a serious loss of particles falling out of the RF bucket. This can be seen in the longitudinal phase space plot shown in Fig. 7.

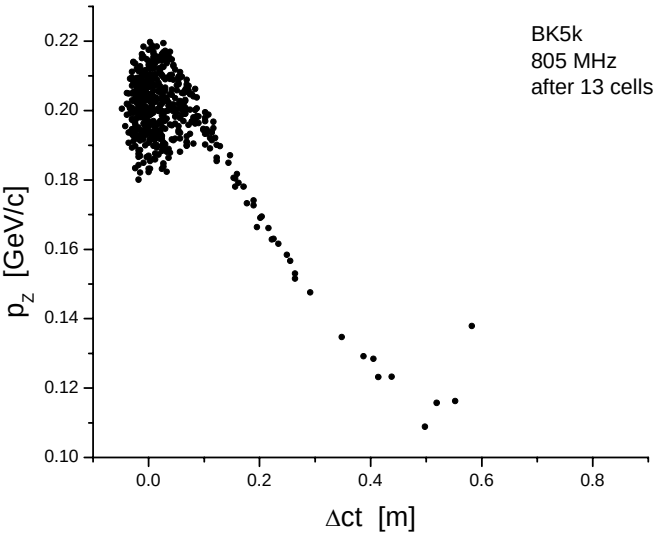

Figure 7. Longitudinal phase space with 805 MHz.

The BK10n reference simulation had a total of 34% losses. It is possible to identify the amount of losses due to particles falling out of the bucket[2] in ICOOL. We found that 20% of the incident particles are lost due to falling out of the RF bucket. Another 10% of the incident particles end up hitting a radial aperture and are still in the bucket. The final 4% are lost due to decays. Comparing this with the results from turning the bucking coil off imply that some coupling must exist between the transverse and longitudinal phase spaces.

It is also clear that the transmission in the LBBC channels is sensitive to initial matching and phase space correlations. Under some conditions it is possible to get good transmission in a bucked channel, as demonstrated for example by the **87%** transmission in the BK20f section of the tapered design in Table 5. On the other hand the beam had 110 m of "conditioning" before it entered this section of lattice.

[2] This was done by setting the BUNCHCUT parameter to 1 ns.

6. Comparison with earlier LBBC designs

The solenoid properties of three previous LBBC designs are given in Table 7. Model a3c5d was designed by Palmer, YS5 by Alexahin, and BCK5 by Fernow.

Table 7 Solenoid properties

model	d	2L	a	t	J	z_b	L_b	a_b	t_b	J_b
	[cm]	[cm]	[cm]	[cm]	[A/mm^2]	[cm]	[cm]	[cm]	[cm]	[A/mm^2]
a3c5d	55.31	22.12	3.95	20.54	184.06	14.22	3.95	3.95	28.44	-179.63
YS5	40	16	3	15	166.6	11	6	3	21	-141.1
BCK5	74	30	5.3	27.3	104.6	19	5	5.3	37.9	-110.1

Models a3c5d and YS5 were designed to achieve a very low beta function in order to reduce the transverse emittance as much as possible. Model BCK5 was designed as a first stage of final cooling following the 805 MHz Guggenheim channel in the HEMC scenario. Some properties of these lattices are given in Table 8.

Table 8 Lattice properties

model	B_o	β_{min}	β_{max}	p_2	Δp_2
	[T]	[cm]	[cm]	[MeV/c]	[MeV/c]
a3c5d	25.5	0.97	35	196	39
YS5	17.0	0.77	25	98	21
BCK5	19.4	1.3	44	200	40

Note that YS5 is unique among the lattices discussed in this report in that the design momentum is ~100 MeV/c and that it alternated the polarity of the focusing solenoids. The cooling performance for these lattices is given in Table 9. All these cooling channels used LiH as the absorber.

Table 9 Cooling channel parameters

model	f_{RF}	G_{RF}	Φ_s	L_{RF}	L_{abs}	N_{cell}	ε_{TN}	ε_{LN}	Tr
	[MHz]	[MV/m]	[^{o}]	[cm]	[cm]		[mm]	[mm]	[%]
a3c5d	805	42	41	14	1.7	147	0.33→0.073	0.48→1.62	54
YS5	800	40	40	8	0.75	66	0.19→0.045	0.21→1.06	36
BCK5	805	40	45	18	2.26	78	0.40→0.14	1.2→2.0	62

Using lattices a3c5d and YS5 after the tapered channel discussed in Table 5 could possibly get the normalized transverse emittance down to ~45 μm at the cost of a further reduction in overall transmission.

7. Ideal emittance exchange

Following the ideas of Palmer [8] we investigated the change in performance if the stages of the tapered channel are separated by ideal solenoidal emittance exchange sections. These sections are used to decrease the momentum spread of the beam and to help prevent particles from falling out of the RF bucket. The emittance exchange is modeled using a 6x6 diagonal transport matrix of the form

$$diagonal\{1, \frac{1}{\sqrt{1-2\delta}}, 1, \frac{1}{\sqrt{1-2\delta}}, 1, 1-2\delta\}$$

where the dimensionless parameter δ determines the strength of the exchange. This matrix transformation has determinant equal to 1 and does not change the value of the 6D emittance. For small values of δ the matrix can be approximated as

$$diagonal\{1, 1+\delta, 1, 1+\delta, 1, 1-2\delta\}$$

At each interface we varied δ in order to optimize the transmission. The resulting tapered channel performance is given in Table 10.

Table 10 Tapered cooling channel with emittance exchange

model	N_{cell}	length	δ	ε_{TN}	ε_{LN}	Tr
		[m]		[mm]	[mm]	[%]
BK10n	45	64.62		0.38	3.4	67.3
BK15f	40	37.60	0.02	0.25	3.8	77.5
BK20f	35	25.17	0.00	0.18	4.2	86.2
BK25e	55	30.80	0.01	0.13	4.6	81.5
Total		**158.2**		**1.01 → 0.13**	**2.0 → 4.6**	**37**

We see that the emittance exchange sections could only provide a slight improvement in the overall transmission. This seems to imply that there is a near-optimal balance between the losses due to falling out of the RF bucket and the transverse losses due to aberrations. Increasing δ by more than a small amount may cause more transverse losses than the reduction it gives in longitudinal losses.

8. Ring configuration

Since a large part of the particle losses in the straight channel is due to particles falling out of the RF bucket, we next examined using a ring configuration. This is another approach for providing emittance exchange to help prevent the growth in longitudinal emittance. On the other hand the resulting dispersion is another cause for increasing the transverse size of the beam and limiting the transverse acceptance.

We examined the BK10n lattice in a ring configuration. Using 24 cells gives a circumference of 34.464 m, which is similar to the circumference of the RFOFO ring. It is simplest to start by assuming a constant dipole field is superimposed over the ring. For a 200 MeV/c reference momentum, this requires a 0.1216 T field. The initial closed orbit parameters are given in Table 11.

Table 11. Initial closed orbit parameters for the BK10n lattice ring.

x_o	y_o	p_{xo}	p_{yo}	p_{zo}
[mm]	[mm]	[MeV/c]	[MeV/c]	[MeV/c]
-18.8	0.2	0.61	-4.05	199.96

The dispersion functions are shown in Fig.8.

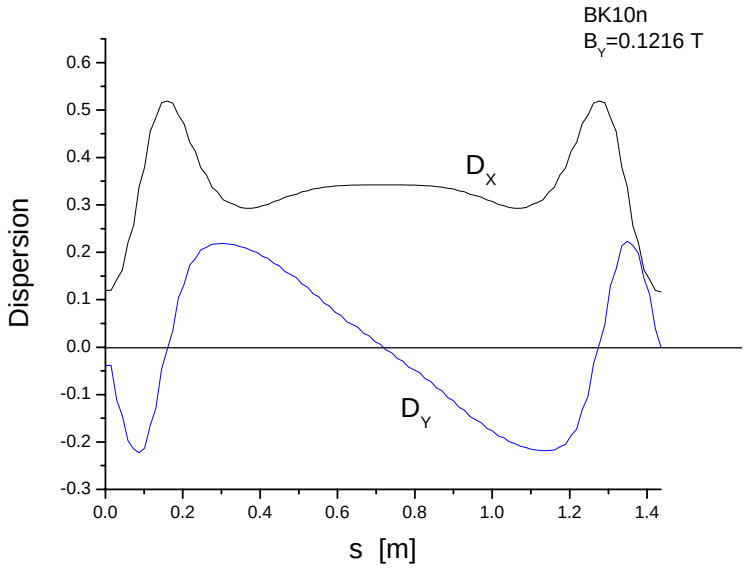

Figure 8. Dispersion functions

The dispersion at the absorber is ~12 cm and is mainly along *x*. The dispersion reaches a maximum value ~52 cm near the end of the focusing coil. Because of the solenoid there is also a component of dispersion in the *y* direction that contributes to the growth of the beam size.

The dispersion prime functions are shown in Fig. 9.

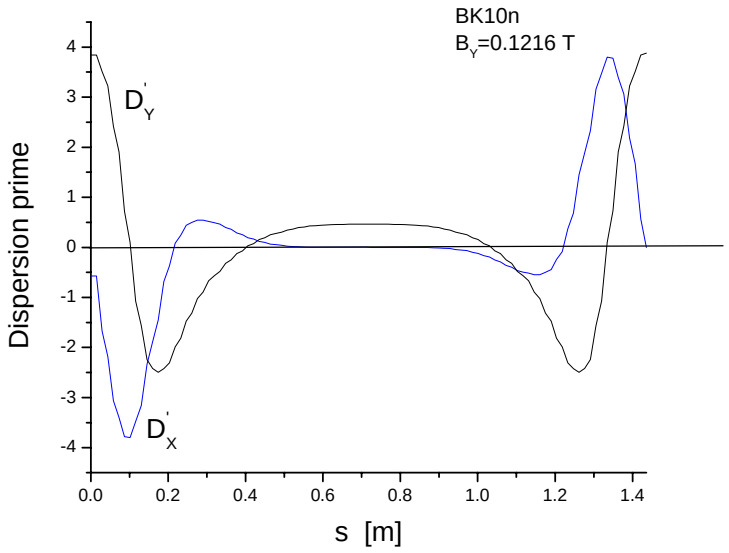

Figure 9. Dispersion prime functions

The dispersion prime at the absorber is ~3.84 and is mainly along *y*.

Initial simulations have been done using both flat absorbers, which use $D_{y'}$, and wedge absorbers, which use D_x. The transmission for both cases was less than half that for the straight 10 T lattice.

9. Conclusions

Low-beta bucked coil lattices offer a backup solution for part of the 6D and final cooling in the HEMC collider scenario. They can efficiently produce low beta functions at the absorbers and simultaneously solve the problem of operating RF cavities in a magnetic field. However, LBBC lattices seem to have an intrinsic problem with transmission losses.

Acknowledgements

I would like to thank Bob Palmer and Yuri Alexahin for useful discussions.

References

[1] R.C. Fernow & R.B. Palmer, Solenoidal ionization cooling lattices, Phys. Rev. STAB 10, 064001 (2007); NFMCC technical note 510, February 2007..

[2] R.C. Fernow, One coil per cell solenoid lattices with the minimum beta function under the coil, NFMCC technical note 508, February 2007.

[3] R.B. Palmer, Lattices, MCTF Thursday Meeting, 14 December 2006.

[4] Y. Alexahin, Study of the "super-Fernow" lattice, MCTF Thursday Meetings, 26 July 2007; 21 February 2008; 29 May 2008.

[5] R. Palmer et al, A complete scheme for a muon collider, Proc. COOL 2007, Bad Kreuznach, Germany, p.77-81; R. Palmer et al, A complete scheme of ionization cooling for a muon collider, Proc. PAC07, Albequerque, New Mexico, p. 3193-3195.

[6] R. Fernow, Bucked cooling channels for the neutrino factory, IDS Workshop, FNAL, June 2008.

[7] C. Rogers, Shielded RF lattice for the muon front end, Proc. NuFact09, July 2009.

[8] R. Palmer, Towards end-to end 6D cooling simulation, talk at MICE Collaboration Meeting, UC Riverside, 24 March 2010.